Journal of Applied Polymer Science

Influence of structure on release profile of acyclovir loaded polyurethane nanofibers: Monolithic and core/shell structures

Maryam Azizi, Mir Saeed Seyed Dorraji, Mohammad Hossein Rasoulifard
Applied Chemistry Research Laboratory, Department of Chemistry, Faculty of Science, University of Zanjan, Iran
Correspondence to: M. S. Seyed Dorraji (E-mail: dorraji@znu.ac.ir) and M. H. Rasoulifard (E-mail: m_h_rasoulifard@znu.ac.ir)

ABSTRACT: In this study, monolithic and core/shell polyurethane (PU) nanofibers were fabricated by single and coaxial electrospinning techniques, respectively. An antivirus drug, Acyclovir (ACY), was loaded on PU nanofibers. The physical condition and interaction of the loaded ACY within these nanofibers were studied by FTIR, XRD, DSC, SEM, and TEM. *In vitro* tests exhibited an obvious difference in the release pattern between monolithic and core/shell nanofibers and burst release in monolithic nanofibers could be controlled by core/shell structure. Release profile was found to follow Korsmeyere-Peppas model with Fickian diffusion mechanism. Our study demonstrated that the ACY-loaded core/shell nanofibers might serve as a device for drug delivery systems. © 2016 Wiley Periodicals, Inc. J. Appl. Polym. Sci. **2016**, *133*, 44073.

KEYWORDS: drug delivery systems; electrospinning; fibers; kinetics

Received 16 March 2016; accepted 11 June 2016
DOI: 10.1002/app.44073

INTRODUCTION

One of the major missions of drug delivery systems is transporting of various drugs to the target positions in the body and adjusting the release mechanisms by controlling the dose of drugs and treatment time in a safe method.[1,2] Several delivery devices have been reported, such as polymeric matrices, gels, foams, film, cyclodextrins and nanofibers each with defined advantages and disadvantages.[3–7] When developing these carriers, the goal is to obtain systems with the least properties, for instance biocompatibility, nontoxicity, biodegradation time, reproducibility, and continuous activation till arrival to the target.[8,9]

Among the various carriers, fibers have been widely used for drug carrier systems due to high surface-area-to-volume ratio, complex porous structure, high loading capacity, ease of operation, flexibility, and cost-effectiveness.[10] One of the most promising techniques to manufacturing of nanofibers with different diameters is electrospinning process because; it is a simple and easy way to control the morphology of ultrafine fibers.[11] The morphology and structure of nanofibers was obtained by electrospinning, were affected by more factors, for example electrospinning process parameters, the polymer solution, and ambient conditions.[12] Nowadays, majority of polymers have been successfully electrospun into ultrafine fibers mostly in solvent solution and some in melt form.[13–15]

Electrospinning from a polymer solution produces medicate fibers with an intense burst release in the initial stage because the most drug compounds, tend to accumulation on or near-surface of the fibers due to the rapid evaporation of the solvent and high ionic strength in solution.[16–18] To overcome this problem, unique fibers with a core/shell structures are offered via polymer solution and coaxial electrospinning to obtain a controlled release profile.[19,20]

Polyurethanes (PU) are extremely versatile materials due to various available uses as polymer for the preparation nanofibers. The advantages of the PU are biocompatibility, excellent tensile strength, chemical resistance, performance in harsh environments, and high moisture vapor transmission rate, which the last case is the most important because of its breathability and softening properties at the body temperature. Due to mentioned properties, PU almost used in the area of medical devices.[21,22] So far, several researchers tried to develop controlled release devices using various polymers and antivirals and investigated *in vitro* or *in vivo* for treatment of skin diseases.[23,24] Among antivirals, Acyclovir (ACY) is one of the oldest drugs that is used to treat herpes simplex viruses and it remains as the first line treatment for these infections.[25,26] The chemical structure of the ACY is presented in Figure 1.

The purpose of this study, firstly, is to prepare various structures of electrospun PU nanofibers, then evaluating *in-vitro*

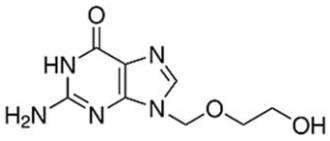

Figure 1. Chemical structure of ACY.

release profile of ACY and comparing release rate of monolithic and core/shell fibers. Another objective of this work is to investigate kind of kinetic models in order to determine the mechanism of drug release.

EXPERIMENTAL

Materials

Biocompatible PU resin (Desmopan 9370A, Bayer Material Science AG) was selected due to its flexible elastomeric properties that make it a suitable candidate material for electrospun drug carrier. Dimethylformamide (DMF) and tetrahydrofuran (THF) were purchased from Merck Chemical (Germany). ACY was a gift from Bakhtar Bioshimi (Iran). The release medium in the drug release test, is Phosphate buffer saline (PBS) tablets (pH = 7.4), which were prepared from Sigma-Aldrich Co. (US). All products were analytical grade and they used without further purifications.

Preparation of Drug-Loaded Fibers

In this study, electrospinning was performed to prepare monolithic (fibers spun with single needle and only one polymer solution) and core/shell (fibers spun with coaxial needle and double polymer solution) fibers.

Electrospinning of Monolithic Fibers. Polymer solutions containing of 8% w/v PU with the model drug (ACY), were prepared in a (50:50) DMF:THF solvent mixtures, while no ACY precipitate was apparent in the polymer solutions. The homogeneous solutions of PU were located in a 5 mL syringe that is fitted with a metallic needle of 0.6 mm inner diameter. The syringe was fixed horizontally on the syringe pump (model: FNM-ES1000, Fanavaran Nano Meghyas, Iran). Electrospinning was carried out by applying a high voltage to the metal needle tip as positive electrode and a fixed sheet of grounded aluminum foil. The parameters of the electrospinning were adjusted as: flow rate = 1.8 mL/h, the critical voltage = 22 kV, the tip-to-collector distance = 200 mm, and during the electrospinning process, the temperature, and relative humidity were maintained at 30 °C and 44–50%, respectively. The collected nanofibers were dried at room temperature and under the fume hood overnight, to evaporate the residual solvent from the nanofibers.

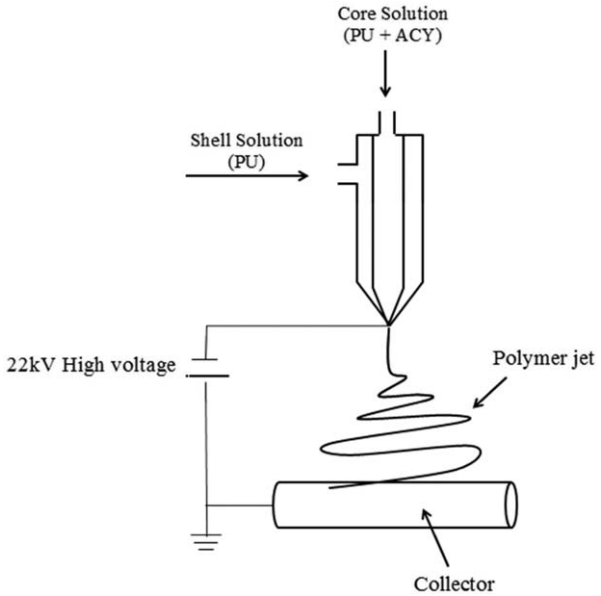

Figure 2. Schematic of coaxial electrospinning.

Electrospinning of Core/Shell Fibers. The basic experimental setup for coaxial electrospinning process is schematically demonstrated in Figure 2. In this procedure, the 8% wt PU solution containing of ACY powders were used as the core material and they were dissolved in a binary solution of (50:50) DMF/THF in volume. The shell material was 8% wt pure PU solution, which were dissolved in their respective solvents. Both the shell and core solutions were fed independently with a programmable syringe pump. The flow rates of both solutions are 0.90 mL/h. An aluminum foil was fitted on a rotating drum that controlled by a step ping motor. A high voltage electric field was applied at the tip of the needle of 22 kV. All the experiments were carried out at 30 °C.

Characterization

Morphological Analysis of Electrospun Fibers. The surface morphologies of the monolithic PU and ACY-loaded PU nanofibers were investigated by using Scanning Electron Microscope (SEM, model: AIS2100, Seron Technology) with an accelerating voltage of 20.0 kV. The morphology of core/shell fibers were observed using Transmission Electron Microscopy.

Structure Characterization. Chemical structures of monolithic, core/shell and pure PU fibers were characterized using Fourier Transform Infrared Spectrophotometer (FTIR, Perkin-Elmer), in the region of 400–4000 cm^{-1} with the resolution of 4 cm^{-1}. The collected spectra were compared each other to emphasis the fact that the core was covered by the shell.

Differential Scanning Calorimetric (DSC) Studies. DSC (METTLER TOLEDO DSC823Greifensee, Switzerland) was used to determine the thermodynamic profiles of electrospun nanofibers. The nature of the drug inside of the nanofibers was investigated by performing DSC on pure drug, pure PU nanofibers, and ACY-loaded nanofibers. Samples (3–7 mg) were heated from 10 to 300 °C at a heating rate of 10 °C/min under a flow of nitrogen (40 mL/min).

X-ray Diffraction (XRD) Analysis. XRD patterns were obtained using (D8 ADVANCE X-ray Diffractometer, Bruker) with

Table I. Explanation of Diffusional Release Mechanism

Release exponent (n)	Drug transport mechanism
$n = 0.45$	Fickian diffusion
$0.45 < n < 0.89$	Non-Fickian transport
$n = 0.89$	Case II transport
$n > 0.89$	Super case II transport

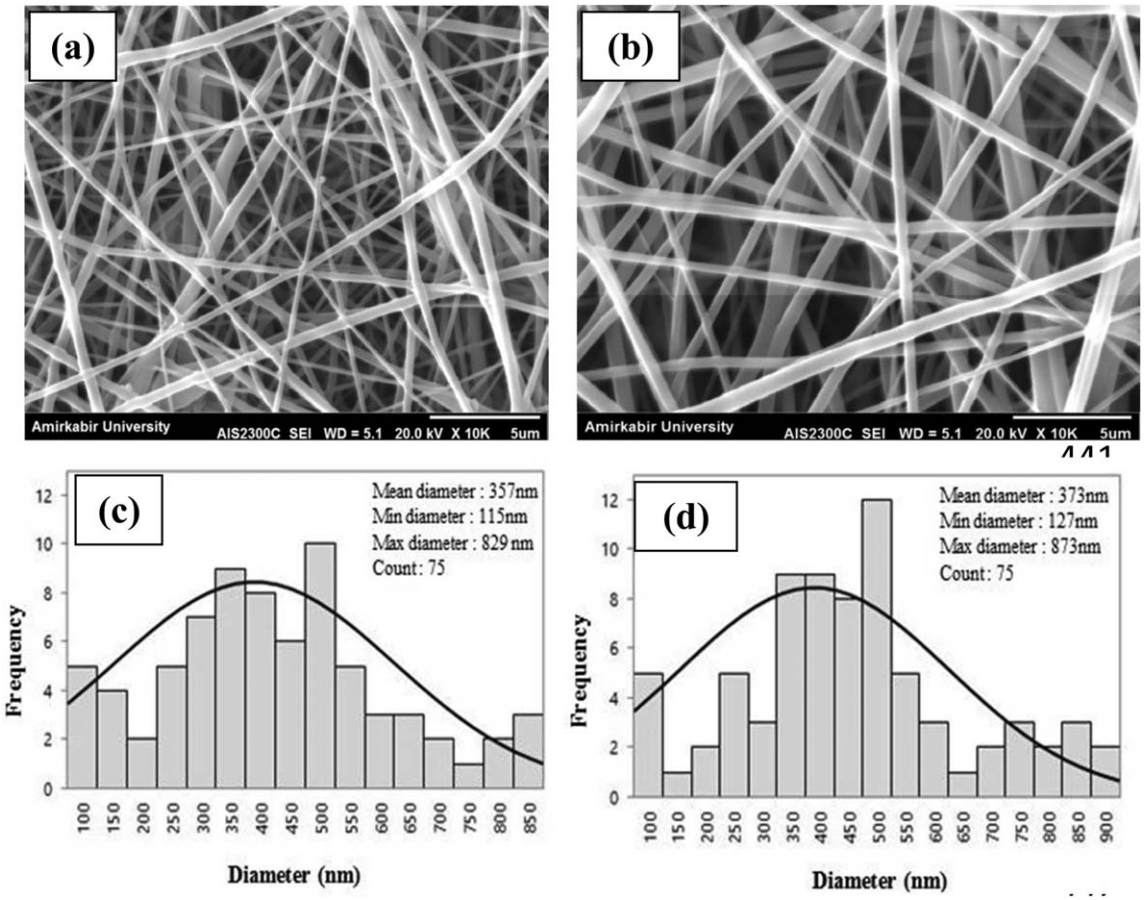

Figure 3. Representative morphologies of electrospun monolithic (a), core/shell nanofibers loaded with ACY (b), and their diameter distribution (c, d).

CuKα radiation in the 2θ ranging from 10 to 75°. The samples were tested under the condition of 40 kV and 300 mA.

In Vitro Drug Release

The release behavior of ACY from monolithic and core/shell nanofibers was investigated via Ultraviolet–visible Spectrophotometry (UV/Vis–1800, Shimadzu) at wavelength of 252 nm. Release tests were performed on the fabricated samples in PBS solution with the conditions of pH 7.4, temperature of 37 ± 0.5 °C and stirring at 150 rpm. The various structures of fibers (15 × 15 cm^2) with the same ACY weight were immersed in 200 mL of the above buffer. The solution was taken out (About 3.5 mL) at scheduled time intervals and it was replenished with an identical volume of fresh buffer medium. The cumulative drug concentration was calculated from the calibration curve of the model drug. The results are explained by percentage of released drug as a function of release time:

$$\text{Cumulative amount of release } (\%) = \frac{M_t}{M_{\text{tot}}} \times 100 \qquad (1)$$

where M_t is the amount of ACY released at certain time (t) and M_{tot} is the total weight of loaded-drug in the nanofibers theoretically. All experiments were collected from triplicate samples.

Kinetics Studies

Different kinetic models (Zero-order, first-order, Higuchi and Korsmeyere-Peppas) were used to determine the kinetics of drug release from fabricated ACY/PU monolithic and core/shell fibers.

Zero Order Model. The release of the drug that confirms zero order kinetics can be represented by the equation[27]:

$$Q_t = k_0 t \qquad (2)$$

where Q_t is the amount of drug released in time t, k_0 is the zero order release constant expressed in units of concentration/time, and t is the time.

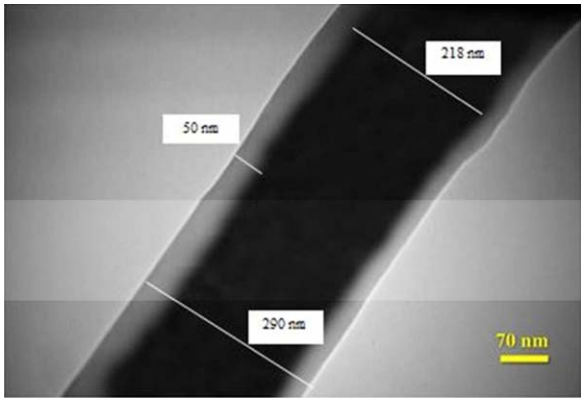

Figure 4. TEM image of core/shell PU nanofibers. [Color figure can be viewed in the online issue, which is available at wileyonlinelibrary.com.]

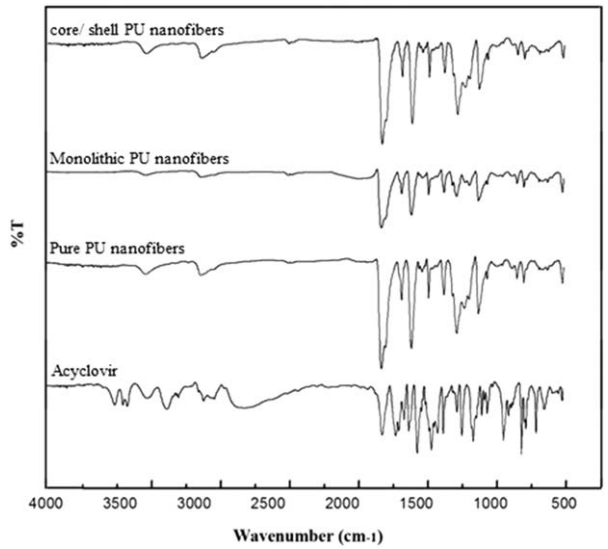

Figure 5. FTIR image of ACY, pure PU nanofibers, monolithic PU nanofibers, and core/shell nanofibers.

First Order Model. First order model, shown in eq. (3), describes the drug release pattern[28]:

$$\mathrm{Log}Q = \mathrm{Log}Q_0 - \frac{kt}{2.303} \tag{3}$$

where Q is the amount of drug released in time t, Q_0 is the initial amount of drug in the solution, and K is the first order release constant.

Higuchi Model. This model describes drug release from nanofibers as a process that is depend on the square root of time, based on Fickian diffusion as in eq. (4)[29]

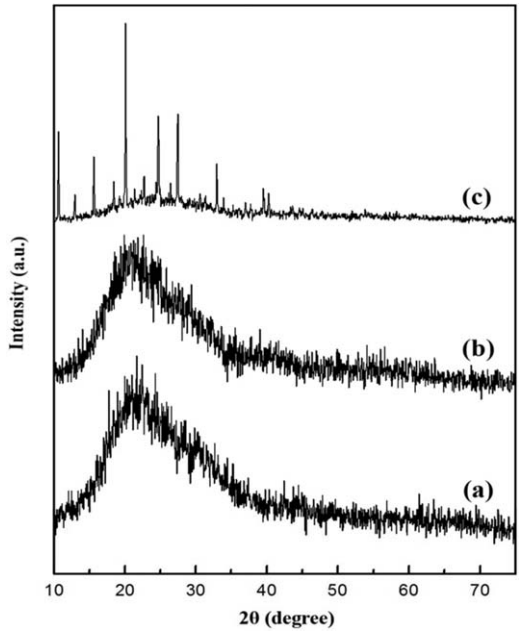

Figure 6. XRD pattern of the (a) Pure PU nanofibers, (b) drug loaded nanofibers, and (c) ACY.

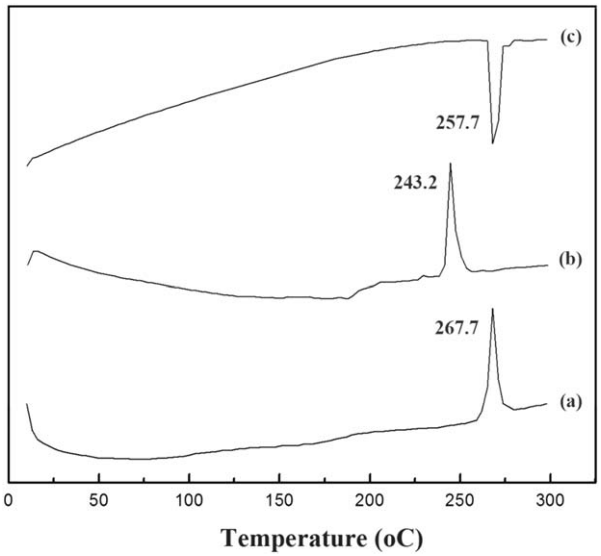

Figure 7. DSC thermograms of the (a) pure PU nanofibers, (b) drug loaded nanofibers, and (c) ACY.

$$Q = kt^{1/2} \tag{4}$$

where, Q is the amount of drug released in time t, and k is the release rate constant for the Higuchi model.

Korsmeyere-Peppas Model. Korsmeyere Peppas is a simple relation, which described drug release from a polymeric system equation. The equation of this model was stated as the following:[30]

$$M_t / M_\infty = kt^n \tag{5}$$

where M_t/M_∞ is a fraction of drug released at time t, k is the release rate constant, and n is the release exponent. The "n" value is used to characterize different release for cylindrical shaped matrices. In this model, the value of "n" characterizes the release mechanism of drug as described in Table I.

RESULTS AND DISCUSSION

Preparation and Morphology of PU Nanofibers

Monolithic and core/shell nanofibers of PU were fabricated by electrospinning process that the procedure of preparing of

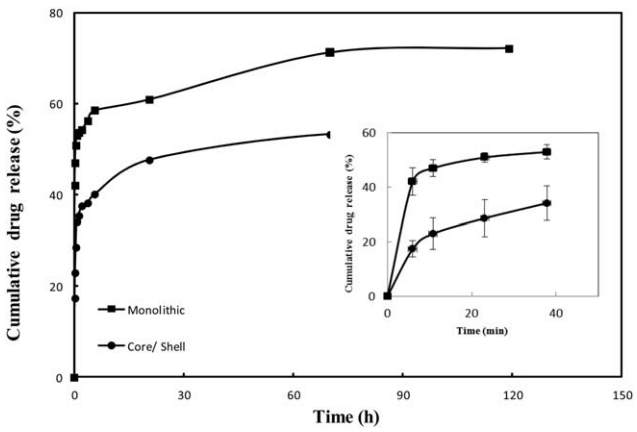

Figure 8. Cumulative release profile of ACY loaded PU nanofibers in PBS, pH 7.4, 37 °C (mean ± SD, $n = 3$).

Table II. Mathematical Modeling of ACY Release from PU Nanofibers

Structure of fibers	R^2				Model parameters		Release mechanism
	Zero	First order	Higuchi	Korsmeyere	*k*	*n*	
Monolithic	0.696	0.673	0.827	0.922	0.546	0.099	Fickian
Core/Shell	0.797	0.737	0.906	0.954	0.368	0.300	Fickian

nanofibers were expressed beforehand. SEM images of the monolithic and core/shell nanofibers are given in Figure 3. The electrospun PU nanofibers loaded with ACY, exhibited smooth surfaces and uniform structures without any beads-on-a-string morphology. The TEM image of core/shell nanofiber was obtained (Figure 4) to confirm the core/shell structure. As shown, there are an keen contrast at the near of the core and shell layers, that this could probably be due to the difference in concentrations and immiscibility of the shell and core solutions, as well as, the fast rate of the electrospinning process that it could forbade the mixture of the two solutions seriously.

Phase Study

To observe the spectral changes and characterize the interaction between the PU nanofibers and ACY, FTIR was exibited in (Figure 5). The broad peak can be seen from the spectrum of Pure ACY at 3436 cm^{-1} due to N—H stretching, also The —C═O absorption peak is observed at 1686.3 cm^{-1}.[31] The spectroscopy of The FTIR spectrum of electrospun PU [Figure 5(b)] shows characteristic absorption bands at 3320, 2960, 1710, 1530, 1220, and 777 cm^{-1}, which represents ν(N—H), ν(C—H), ν(C═O), ν(C—C), ν(C—C), and ν(C—H), respectively.[32] The results show that the core/shell fibers are resemble to one of that monolithic fibers of the shell polymers without loaded drug. The spectra of monolithic nanofibers loaded with ACY [Figure 5(c)] are analogous with the spectra of pure nanofibers [Figure 5(b)]. It can be inferred that no chemical reaction of polymer and drug occurred or it may be could not be detected by FTIR, due to only 1.2% drug loaded on the nanofibers.[33]

X-ray diffraction pattern of ACY, pure electrospun PU and PU-nanofibers loaded with drug were displayed in Figure 6 that they discribe the distribution and physical situation of ACY in the electrospun PU nanofibers. It shows that PU nanofibers have typical broad peak around $2\theta = 20°$ whereas they are amorphous polymeric in nature. We also observed drug loaded nanofibers with the same peak while ACY drug were exhibited as crystalline materials with characteristic peaks at 2θ of 10.4°, 23.2°, 26.0°, and 29.1°.[31] Therefore, we concluded that drug was loaded in amorphous mode in the electrospun PU nanofibers, also there was no any strong interaction between PU and ACY.

The Thermal studies of ACY, pure nanofibers and ACY-loaded electrospun nanofibrous are shown in Figure 7. The profile for pure nanofibers exhibits a broad exothermic peak at 267.7 °C. The DSC curve of ACY displays an endothermic peak at 257.7 °C corresponding to its melting temperature,[34] while, no peak detected on the DSC thermograms of ACY loaded electrospun nanofibrous in this region [Figure 7(b)], so the ACY was in amorphous state in the PU nanofibers. A weakened interaction between PU and ACY lead to the peak temperatures of pure nanofibers was shifted slightly to a lower temperature (243.2 °C). These results are supported by conclusion of XRD analysis.

Drug Release from Nanofibers

The ACY release profiles from prepared PU nanofibers with various structures are given in Figure 8. The results illustrate that the ultimate release percentage of ACY from monolithic nanofibers (electrospun from single solution) is about 75%, while they have a certain amount of drug release at 30 min (as initial burst released), which may be imputed to the more propensity to accumulation of ACY to the surface or near-surface of nanofibers during the electrospinning process. With focusing on the effect of the fiber structure on the release profiles, and comparing the release profiles of ACY from PU monolithic fibers with core/shell nanofibers, it is believed that using of core/shell structure affects the release behavior due to conceal drug on the surface nanofibers by shell. Thus, this process can be one of the ways to overcome burst release of monoliths nanofibers.

Drug Delivery Kinetics

Release kinetics of the ACY from monolithic and core/shell PU nanofibers were determined by fitting drug release data with the zero order, first order, Higuchi, and Korsmeyere-Peppas models. The evaluated kinetic release parameters were listed in Table II. Results of these analyses show the poor fit of the experimental data into the zero order, first order, Higuchi equation ($R^2 < 0.98$), whereas Korsmeyere-Peppas model gives the closest fits to the experimental results, with R^2 values of >0.9.

The fact that degradation of PU is very lentamente in aqueous medium due to its amorphous and hydrophobic nature that leads to the ACY release from different structure of nanofibers followed Fickian diffusion mechanism.

CONCLUSIONS

In this experiment, ACY loaded PU nanofibers were fabricated and their release profiles were compared with those of core/shell fibers made from the similar polymers. The physical condition and interaction of the loaded ACY within these nanofibers were confirmed using FTIR, XRD, and DSC analysis. The *in vitro* release tests in phosphate buffer with pH 7.4 showed that the PU monolithic fibers had initial burst release, while this phenomenon could be controlled by core/shell structure of PU nanofibers. Conclusively, this study proposed the effective method to overcome burst release, so it should be used in medical applications due to sustaining drug release for a prolonged period of time.

ACKNOWLEDGMENTS

The authors thank the University of Zanjan, Iran for financial and other supports.

REFERENCES

1. Allen, T. M.; Cullis, P. R. *Science* **2004**, *303*, 1818.
2. Frandsen, J. L.; Ghandehari, H. *Chem. Soc. Rev.* **2012**, *41*, 2696.
3. Wolinsky, J. B.; Colson, Y. L.; Grinstaff, M. W. *J. Control. Release* **2012**, *159*, 14.
4. Canbolat, M. F.; Celebioglu, A.; Uyar, T. *Colloids Surf. B* **2014**, *115*, 15.
5. Zhang, Y.; Zhang, J.; Jiang, T.; Wang, S. *Int. J. Pharm.* **2011**, *410*, 118.
6. Li, J.; Loh, X. J. *Adv. Drug Delivery Rev.* **2008**, *60*, 1000.
7. Hung, S. F.; Hsieh, C. M.; Chen, Y. C.; Wang, Y. C.; Ho, H. O.; Sheu, M. T. *PLoS One* **2014**, *9*, e100321.
8. Palombo, M.; Deshmukh, M.; Myers, D.; Gao, J.; Szekely, Z.; Sinko, P. J. *Annu. Rev. Pharmacol.* **2014**, *54*, 581.
9. De Koker, S.; Hoogenboom, R.; De Geest, B. G. *Chem. Soc. Rev.* **2012**, *41*, 2867.
10. Agarwal, S.; Wendorff, J. H.; Greiner, A. *Polymer* **2008**, *49*, 5603.
11. Greiner, A.; Wendorff, J. H. *Angew. Chem. Int. Ed.* **2007**, *46*, 5670.
12. Beachley, V.; Wen, X. *Mater. Sci. Eng. C* **2009**, *29*, 663.
13. Wang, H.; She, Y.; Chu, C.; Liu, H.; Jiang, S.; Sun, M.; Jiang, S. *J. Mater. Sci.* **2015**, *50*, 5068.
14. Wu, Y. H.; Yu, D. G.; Li, X. Y.; Diao, A. H.; Illangakoon, U. E.; Williams, G. R. *J. Mater. Sci.* **2015**, *50*, 3604.
15. Yan, J.; White, K.; Yu, D. G.; Zhao, X. Y. *J. Mater. Sci.* **2014**, *49*, 538.
16. Cui, W.; Zhou, Y.; Chang, J. *Sci. Technol. Adv. Mater.* **2010**, *11*, 014108.
17. Li, X.; Kanjwal, M. A.; Lin, L.; Chronakis, I. S. *Colloids Surf. B* **2013**, *103*, 182.
18. Natu, M. V.; de Sousa, H. C.; Gil, M. *Int. J. Pharm.* **2010**, *397*, 50.
19. Dror, Y.; Salalha, W.; Avrahami, R.; Zussman, E.; Yarin, A.; Dersch, R.; Greiner, A. *J. Wendorff Small* **2007**, *3*, 1064.
20. Tiwari, S. K.; Tzezana, R.; Zussman, E.; Venkatraman, S. S. *Int. J. Pharm.* **2010**, *392*, 209.
21. Saha, K.; Butola, B. S.; Joshi, M. *J. Appl. Polym. Sci.* **2014**, *131*, 40824. DOI: 10.1002/app.
22. Piozzi, A.; Francolini, I.; Occhiaperti, L.; Venditti, M.; Marconi, W. *Int. J. Pharm.* **2004**, *280*, 173.
23. Manne, N.; Yadav, H. K.; Kumar, S. H.; Khom, T. C.; Kumar, N. S. *J. Appl. Polym. Sci.* **2014**, *131*, DOI: 10.1002/app.
24. Singh, B.; Bala, R. *Chem. Eng. Res. Des.* **2012**, *90*, 346.
25. Chaudhary, B.; Verma, S. *Sci. World J.* **2014**, *2014*, 280928.
26. Mali, N.; Jadhav, S.; Karpe, M.; Kadam, V. *Int. J. Pharm. Pharm. Sci.* **2011**, *3*, 45.
27. Chatzaeiaoannou, T. Quantitative Calculations in Pharmaceutical Practice and Research; VCH Publishers: New York, **1993**.
28. Singhvi, G.; Singh, M. *Int. J. Pharm. Stud. Res.* **2011**, *2*, 77.
29. Lokhandwala, H.; Deshpande, A.; Deshpande, S. *Int. J. Pharm. Bio. Sci.* **2013**, *4*, 728.
30. Dash, S.; Murthy, P. N.; Nath, L.; Chowdhury, P. *Acta Pol. Pharm.* **2010**, *67*, 217.
31. Chen, H. M.; Yu, D. G. *J. Mater. Process Tech.* **2010**, *210*, 1551.
32. Jiang, Z.; Yuan, K.; Li, S.; Chow, W. *Spectrosc. Spect. Anal.* **2006**, *26*, 624.
33. Ma, G.; Liu, Y.; Peng, C.; Fang, D.; He, B.; Nie, J. *Carbohydr. Polym.* **2011**, *86*, 505.
34. Yu, D. G.; Branford-White, C.; Li, L.; Wu, X. M.; Zhu, L. M. *J. Appl. Polym. Sci.* **2010**, *117*, 1509.